MOLECULAR BIOLOGY

Precise correction of Duchenne muscular dystrophy exon deletion mutations by base and prime editing

F. Chemello[1,2,3†], A. C. Chai[1,2,3†], H. Li[1,2,3†], C. Rodriguez-Caycedo[1,2,3], E. Sanchez-Ortiz[1,2,3], A. Atmanli[1,2,3], A. A. Mireault[1,2,3], N. Liu[1,2,3], R. Bassel-Duby[1,2,3], E. N. Olson[1,2,3]*

Duchenne muscular dystrophy (DMD) is a fatal muscle disease caused by the lack of dystrophin, which maintains muscle membrane integrity. We used an adenine base editor (ABE) to modify splice donor sites of the dystrophin gene, causing skipping of a common DMD deletion mutation of exon 51 (ΔEx51) in cardiomyocytes derived from human induced pluripotent stem cells, restoring dystrophin expression. Prime editing was also capable of reframing the dystrophin open reading frame in these cardiomyocytes. Intramuscular injection of ΔEx51 mice with adeno-associated virus serotype-9 encoding ABE components as a split-intein trans-splicing system allowed gene editing and disease correction in vivo. Our findings demonstrate the effectiveness of nucleotide editing for the correction of diverse DMD mutations with minimal modification of the genome, although improved delivery methods will be required before these strategies can be used to sufficiently edit the genome in patients with DMD.

INTRODUCTION

Duchenne muscular dystrophy (DMD) is a fatal X-linked recessive disorder of progressive neuromuscular weakness and wasting, caused by mutations in the *DMD* gene that encodes the dystrophin protein (*1*). While there are thousands of documented clinical mutations, most DMD-causing mutations occur in a "hotspot" region encompassing exons 45 to 55 of the *DMD* gene that encodes the central rod domain of the protein (*2*). Mutations in the *DMD* gene most commonly involve single- or multi-exon deletions that disrupt the open reading frame (ORF) and introduce a premature stop codon that results in the production of a nonfunctional truncated dystrophin protein and causes a severe muscle degeneration phenotype (*3*).

Our laboratory and others have demonstrated the use of myoediting, defined as the CRISPR-Cas9 genome editing in muscle, to permanently correct DMD mutations. Myoediting restores the production of a truncated but functional dystrophin protein in human induced pluripotent stem cell (iPSC)–derived cardiomyocytes, mouse models, and large animal models with DMD mutations (*4*–*10*). These myoediting strategies aimed to "reframe" the correct ORF of the dystrophin transcript by introducing small insertions and deletions (INDELs) via nonhomologous end joining (NHEJ) of double-stranded DNA breaks (DSBs) generated by CRISPR-Cas9. Restoration of the ORF was also accomplished via exon skipping by using a single-guide RNA (sgRNA) that introduces large INDELs by a "single cut" at a splice acceptor site (SAS) or splice donor site (SDS) or by using two sgRNAs to introduce a "double cut" and remove one or more exons (*11*).

The engineered CRISPR technologies of base editing and prime editing have expanded the toolbox of gene editing strategies to potentially correct genetic mutations by enabling precise edits at individual nucleotides (*12*). In base editing, Cas9 nickase (nCas9) or deactivated Cas9 (dCas9) is fused to a deaminase protein, allowing precise single–base pair conversions without DSBs within a defined editing window in relation to the protospacer adjacent motif (PAM) site of an sgRNA (*13*). There are two major classes of DNA base editors: cytosine base editors (CBEs), which convert a C:G base pair into a T:A base pair, and adenine base editors (ABEs), which convert an A:T base pair into a G:C base pair. Recently, an ABE (ABE7.10) was used to introduce a point mutation and a premature stop codon (p.Q871X) in exon 20 of the mouse *Dmd* gene and to correct that same point mutation (*14*, *15*). In addition to correcting point mutations, base editors can also be used to induce exon skipping by mutating target DNA bases of splice motifs (*16*). In this regard, a CBE (hAID P182X) was used at various canonical intronic motifs to modulate splicing of different genes, including the *DMD* gene in DMD patient–derived iPSCs (*17*). However, CBEs have been reported to introduce Cas-independent off-target editing at both the genome and transcriptome levels (*18*–*21*).

The prime editing system is composed of a prime editing guide RNA (pegRNA) and a nCas9 fused to an engineered reverse transcriptase (*22*). The pegRNA consists of an sgRNA (from 5′ to 3′) that anneals to a target site, a scaffold for the nCas9, a reverse transcription template (RT template) containing the desired edit, and a primer binding site (PBS) that binds to the nontarget strand. The RT template can be programmed to introduce any type of edit, including all possible base transitions and transversions, and insertions and deletions of nucleotides of any length. The prime editing system is further enhanced by including an additional nicking sgRNA that increases editing efficiency by favoring DNA repair to replace the non-edited strand. Notably, prime editing has not been previously demonstrated as a gene editing correction strategy for DMD.

In this study, we developed nucleotide gene editing correction strategies to restore dystrophin expression in mice and human cardiomyocytes harboring a deletion of exon 51 (ΔEx51) of the *DMD* gene, one of the most common single-exon deletion mutations in patients with DMD (*23*). We demonstrate the use of an optimized ABE [ABEmax (*24*)] packaged into adeno-associated virus 9 (AAV9) using a split-intein system to restore dystrophin protein expression in a ΔEx51 DMD mouse model, in which correction strategies have not previously been described. We then validate the efficacy of ABEmax for exon skipping in the *DMD* gene locus by

[1]Department of Molecular Biology, University of Texas Southwestern Medical Center, Dallas, TX 75390, USA. [2]Hamon Center for Regenerative Science and Medicine, University of Texas Southwestern Medical Center, Dallas, TX 75390, USA. [3]Senator Paul D. Wellstone Muscular Dystrophy Cooperative Research Center, University of Texas Southwestern Medical Center, Dallas, TX 75390, USA.
*Corresponding author. Email: eric.olson@utsouthwestern.edu
†These authors contributed equally to this work.

targeting SDSs and the efficacy of prime editing for exon reframing in human ΔEx51 DMD iPSCs. Both of these gene editing tools restored the ORF of the dystrophin transcript and rescued dystrophin protein expression. These proposed correction strategies for the ΔEx51 mutation could theoretically restore the correct ORF in ~8% of patients with DMD (*25*). However, the use of a high viral dose to restore in vivo dystrophin expression precludes safe therapeutic deployment of these strategies without further evaluation of dose titration or the effects of systemic treatments. Our findings establish the proof of concept of two nucleotide editing strategies to correct exon deletion mutations in the *DMD* gene through the most minimal possible genomic modifications, resulting in restoration of dystrophin protein expression.

RESULTS

Development of "single-swap" ABE as an in vivo nucleotide editing strategy

Previously, we generated and validated a DMD mouse model with deletion of exon 51 in the mouse *Dmd* gene (ΔEx51) (*26*). These mice display the hallmarks of DMD, including the absence of dystrophin, replacement of degenerative muscle fibers with inflammatory cells and fibrotic and fatty tissue, and an increased percentage of centralized nuclei in myofibers, indicative of active myofiber degeneration and regeneration. Deletion of exon 51 in the *Dmd* gene results in the introduction of a downstream premature stop codon in exon 52 and production of a nonfunctional truncated dystrophin protein (Fig. 1A, top). The *Dmd* ORF can be restored by skipping of either exon 50 or 52. This allows splicing of exons 49 to 52 in the case of exon 50 skipping or splicing of exons 50 to 53 in the case of exon 52 skipping (Fig. 1A, exon skipping). Another correction strategy involves "reframing" of exon 50 or 52 by targeted nucleotide base pair insertions or deletions. Accordingly, insertions of 3n + 2 nucleotides (nt) or deletions of 3n − 1 nt within exon 50 or 52 can restore the ORF (Fig. 1A, reframing). However, these INDELs must occur at sites in the exon that do not result in introduction of a new premature stop codon following the targeted insertions or deletions. Both correction strategies can restore the ORF and lead to production of a functional but internally truncated dystrophin protein.

To restore dystrophin expression in the ΔEx51 mouse model, we decided to induce exon skipping by destroying the SAS or SDS of exon 50 or 52 by a single-swap base pair transition using base editing. The canonical SAS consensus sequence is AG, and the canonical SDS consensus sequence is GT, and the pairing of the SAS and SDS defines an exon for recognition by the splicing machinery (*27*). ABEs can disrupt either the SAS or SDS consensus sequences by causing a single swap of one of the base pairs in the dinucleotide splicing motifs. We reasoned that destruction of either splice site bracketing exon 50 or 52 could prevent pairing of the splice sites across that exon by the splicing machinery. This would preclude the splicing machinery from recognizing that exon, thereby causing skipping of that exon and restoring the correct ORF of the *Dmd* transcript.

For exon skipping in ΔEx51 mice, we used the ABEmax ABE, as ABEs produce less off-target editing than CBEs (*18*–*21*). ABEmax can edit the adenine in the sense strand of the SAS AG consensus sequence or the adenine in the antisense strand of the SDS GT consensus sequence. We identified candidate sgRNAs around the SAS and SDS for both exons 50 and 52 that had PAMs with an NGG PAM sequence for editing with ABEmax-SpCas9 or the more relaxed NG PAM sequence for editing with the engineered ABEmax-SpCas9-NG (*28*). These sgRNAs also positioned the target SAS or SDS within the canonical base editing window of ABEmax (approximatively nucleotide positions 12 to 18; counting the PAM nucleotides as −2 to 0 for NGG or −1 to 0 for NG).

We tested a total of nine candidate sgRNAs in mouse N2a neuroblastoma cells targeting either the SAS or SDS of exon 50 or 52 (fig. S1A). We found that mouse exon 50 (mEx50) sgRNA-4 together with ABEmax-SpCas9-NG was the most efficient sgRNA overall (Fig. 1B and fig. S1B). mEx50 sgRNA-4 induced on-target editing of position A14 of 51.0 ± 2.3% in the SDS of exon 50, with minor

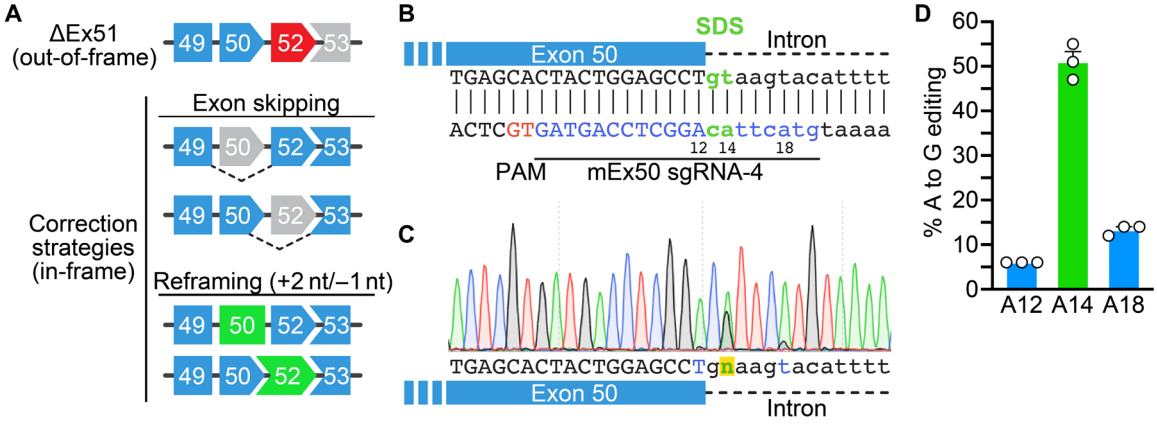

Fig. 1. Strategy for in vivo exon skipping mediated by adenine base editing in the ΔEx51 mouse model. (**A**) Schematic showing exon skipping and exon reframing strategies to restore the correct ORF of the *Dmd* transcript. Shape and color of boxes of *Dmd* exons indicate reading frame. Deletion of exon 51 (ΔEx51) in the *Dmd* gene generates a premature stop codon in exon 52 (red). Restoration of the correct ORF can be obtained by skipping of exon 50 or 52 (gray) or reframing by a precise insertion of 3n + 2 nt or deletion of 3n − 1 nt in exon 50 or 52 (green). (**B**) Illustration of the mEx50 sgRNA-4 binding position in the region of the SDS (green) of mouse *Dmd* exon 50. Sequence shows sgRNA (blue) and PAM (red). Adenines in the editable window of ABEmax-SpCas9-NG are numbered, starting from the PAM. (**C**) Representative Sanger sequencing chromatogram of the genomic region of the exon 50 SDS in mouse N2a cells, after transfection with ABEmax-SpCas9-NG and mEx50 sgRNA-4. (**D**) Percentages of DNA editing in mouse N2a cells after transfection with ABEmax-SpCas9-NG and mEx50 sgRNA-4. On-target edit (A14) is colored green. Dots and bars represent different transfection experiments and are means ± SEM ($n = 3$).

bystander editing at A12 and A18 (Fig. 1, C and D). The other candidate sgRNAs showed low editing efficiency at on-target sites (fig. S1B). We therefore selected mEx50 sgRNA-4 with ABEmax-SpCas9-NG for further in vivo base editing studies.

AAV packaging of ABE components in a split-intein system for in vivo delivery

Current viral-based gene editing therapies use AAVs that have a packaging limit of <5 kb, which precludes packaging of the ABEmax-SpCas9-NG base editor (~5.8 kb) into a single AAV vector. Recently, dual AAVs have been described for the delivery of split base editors using trans-splicing inteins, which act as protein introns to enable covalent splicing of N- and C-terminal peptides (*29*). Each half of the split base editor when linked to trans-splicing inteins can reassemble after translation into a functional base editor that retains similar editing efficiencies compared to its nonsplit, full-length equivalent.

We adapted the split-intein system by dividing ABEmax-SpCas9-NG into two smaller fragments that can each be packaged within separate AAV vectors (Fig. 2A). The N-terminal AAV construct consisted of the N-terminal half of ABEmax-SpCas9-NG fused to one split DnaE intein half from *Nostoc punctiforme* (Npu) that was expressed under the control of the creatine kinase 8 (CK8e) promoter. This promoter drives high level expression specifically in skeletal muscle and heart (*30*). The C-terminal AAV construct consisted of the other DnaE intein half from Npu fused to the C-terminal half of ABEmax-SpCas9-NG, also driven by the CK8e promoter. Each AAV construct also contained a truncated Woodchuck hepatitis virus posttranscriptional regulatory element (WPRE3) (*31*), two codon-optimized nuclear localization signals each flanking the ABEmax-SpCas9-NG halves, and a U6-driven sgRNA in the reverse orientation. We then generated dual-AAV9 particles encoding each of the terminal halves and mEx50 sgRNA-4 (Fig. 2A).

Single-swap ABE in ΔEx51 mice by AAV9 delivery restores dystrophin production

To validate the efficacy of the single-swap gene editing strategy in the ΔEx51 mouse model using ABEmax-SpCas9-NG and mEx50

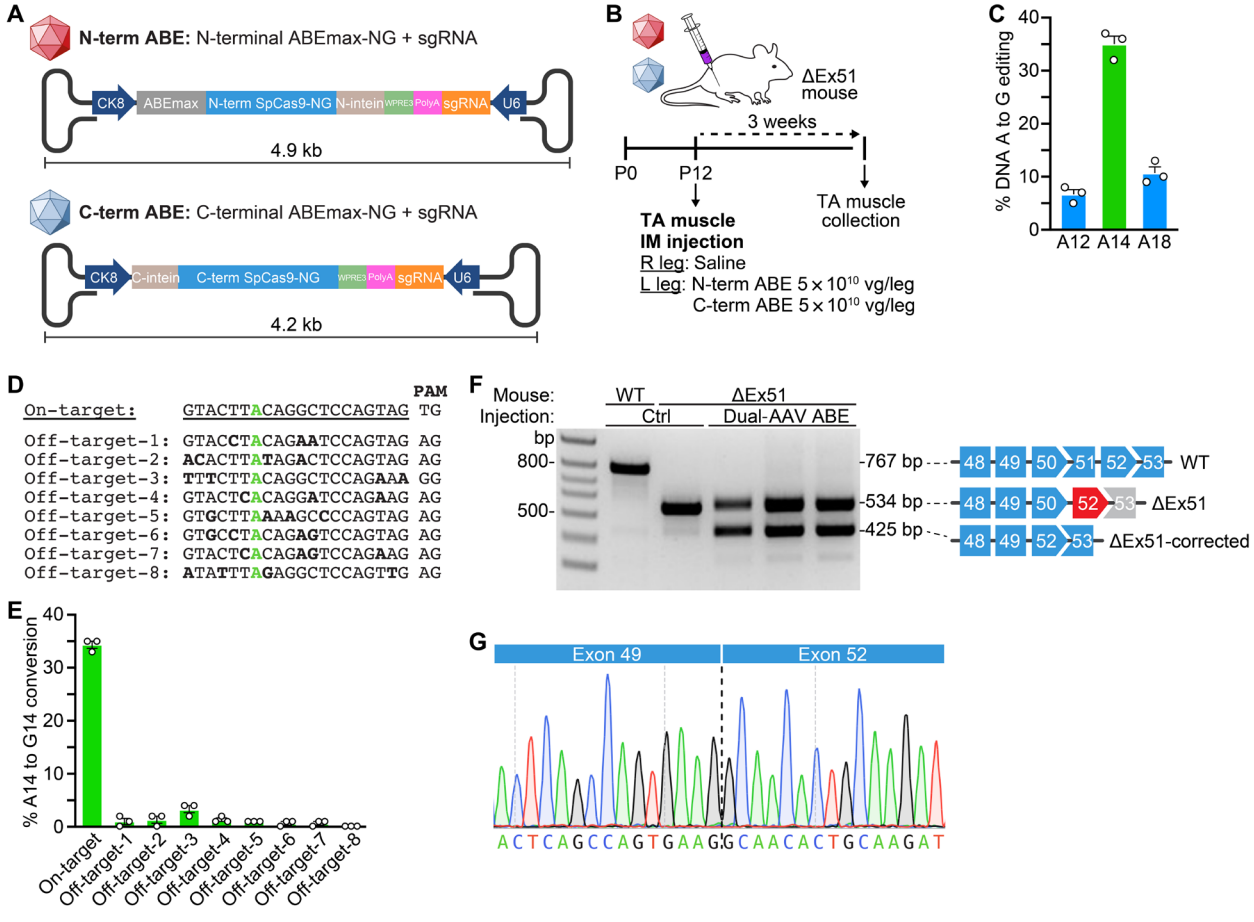

Fig. 2. Exon skipping by AAV-mediated base editing in the ΔEx51 mouse model. (**A**) Schematic of the dual-AAV9 system for in vivo delivery of ABEmax-SpCas9-NG and two copies of mEx50 sgRNA-4. (**B**) Overview for the in vivo intramuscular (IM) injection of the dual-AAV9 system in the TA muscle of the left leg of P12 ΔEx51 mice. Right leg was injected with saline as a control. (**C**) Percentages of DNA editing of the adenines from TA injected with the dual-AAV9 system. On-target adenine (A14) is colored green. Dots and bars represent biological replicates and are means ± SEM ($n = 3$). (**D**) Alignment of the top eight off-target sites in mouse DNA. The target adenine (A14) is colored green. (**E**) Percentages of DNA editing of A14 in the top eight off-target sites from TA injected with the dual-AAV9 system. Dots and bars represent biological replicates and are means ± SEM ($n = 3$). (**F**) RT-PCR analysis of RNA from the TA of wild-type (WT) and ΔEx51 mice injected with the dual-AAV9 system or saline as control (Ctrl). (**G**) Sequence of the RT-PCR product of the lower band confirms splicing of exons 49 to 52.

sgRNA-4, we performed localized intramuscular injection of the dual-AAV9 split-intein system in the left tibialis anterior (TA) muscle [5×10^{10} viral genomes (vg) per leg for each virus] of postnatal day 12 (P12) mice. The right TA muscle was injected with saline solution as a control. Three weeks after intramuscular injection, TA muscles were collected for analyses (Fig. 2B).

Sequencing of genomic DNA in the treated left leg showed an efficiency of on-target editing of A14 of 35.0 ± 1.5%, with bystander editing at A12 of 6.7 ± 0.9% and at A18 of 10.7 ± 1.2% (Fig. 2C). To assess the specificity of base editing, we screened for potential off-target editing of the top eight sites predicted by CRISPOR (Fig. 2D) (*32*). Sequence analysis of the candidate off-target amplicons revealed no notable editing at any of the eight tested off-target sites (Fig. 2E and fig. S2, A and B).

Sequencing of the RT-PCR (polymerase chain reaction) products generated by primers that amplified the region from exon 48 to 53 from the injected TA muscle revealed skipping of exon 50 in mature *Dmd* mRNA (Fig. 2F, lower band). Skipping of exon 50 allows exon 49 to splice to exon 52 and places the downstream *Dmd* transcript back in frame (Fig. 2G). Accordingly, Western blot analysis showed restoration of dystrophin protein expression in the AAV-injected TA muscle to a level of 54.0 ± 1.7% compared to wild-type (WT) littermate controls (Fig. 3, A and B). Immunohistochemistry showed that dystrophin expression was restored in 96.5 ± 0.7% of myofibers (Fig. 3C and fig. S3, A and B). Histological analysis by hematoxylin and eosin (H&E) staining showed substantial reduction in fibrosis, necrotic myofibers, and regenerating fibers with a reduction in centralized nuclei from 51.5 ± 2.8 to 5.9 ± 1.1%, demonstrating amelioration of the DMD phenotype (Fig. 3D and fig. S4, A to C). Collectively, these data demonstrate that exon skipping mediated by base editing can restore dystrophin expression in developing P12 ΔEx51 mouse TA muscles following intramuscular injection of AAV9 at a dose similar to previously published studies (*4*, *8*, *9*, *15*, *33*, *34*). The amount of AAV9 used in this study pertains specifically to intramuscular injection. As our work represents a proof-of-concept study, we do not recommend extrapolating this AAV dose to systemic application, as it would correspond to ~1.5×10^{16} vg/kg and would be an inappropriate amount of virus to administer systemically.

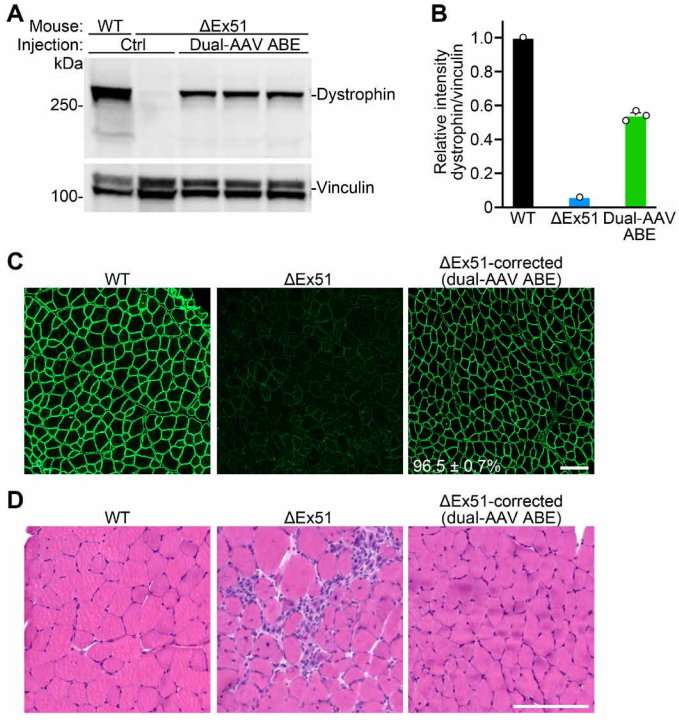

Fig. 3. Dystrophin restoration following AAV-mediated base editing in the ΔEx51 mouse model. (**A**) Western blot analysis of dystrophin protein expression in TA muscles of WT and ΔEx51 mice 3 weeks after intramuscular injection of saline as control (Ctrl) or the dual-AAV9 system for the expression of ABEmax-SpCas9-NG and mEx50 sgRNA-4. Vinculin is the loading control. (**B**) Quantification of dystrophin expression from Western blots after normalization to vinculin. Dots and bars represent biological replicates and are means ± SEM ($n = 3$). (**C**) Immunohistochemistry of dystrophin in TA muscles 3 weeks after intramuscular injection of the dual-AAV9 system. Indicated is the percentage (means ± SEM) of dystrophin-positive myofibers of TA muscles of ΔEx51 mice receiving an intramuscular injection of the dual-AAV9 system ($n = 3$). Dystrophin is indicated in green. Scale bar, 100 μm. (**D**) H&E staining of TA muscles from WT, ΔEx51, and corrected ΔEx51 mice 3 weeks after intramuscular injection. Scale bar, 100 μm.

A single-swap ABE transition induces exon skipping and restores dystrophin expression in human cardiomyocytes

Correction of the *DMD* exon 51 deletion mutation by skipping of exon 50 or 52 can therapeutically benefit ~8% of patients with DMD (*25*). To test whether the single-swap gene editing strategy that we validated in mice was therapeutically translatable to human iPSC-derived cardiomyocytes, we first generated exon 51–deleted human iPSCs. Starting with an iPSC line generated from a healthy male donor, we used CRISPR-Cas9 genomic editing to generate an isogenic disease-specific human iPSC line (ΔEx51 iPSCs) with a deletion of exon 51 in the *DMD* gene (fig. S5). This isogenic pair lessens the possibility of potential intrinsic variations between individual iPSC lines that could lead to misinterpretation of disease-relevant phenotypes (*35*, *36*).

To evaluate the efficiency of base editing of splice sites within the *DMD* gene by the ABEmax base editor, we screened available sgRNAs with NGG PAMs for editing of the SDS or SAS of exon 50 or 52 in human 293T cells. We identified one sgRNA for the SDS of human exon 50 (hEx50 sgRNA-1), which has high homology to mEx50 sgRNA-4 used for the previous mouse in vivo experiments, and two sgRNAs for the SAS of human exon 52 (hEx52 sgRNA-2 and sgRNA-3) that positioned the SAS or SDS within the editing window of ABEmax (Fig. 4, A and B, and fig. S6A).

In human 293T cells, hEx50 sgRNA-1 paired with ABEmax-SpCas9 was the most efficient combination of ABE components, with on-target editing of the A:T to G:C base pair in the SDS GT sequence of 38 ± 0.6% (nucleotide position A14) and bystander edits of 2.0 ± 0.0 and 11 ± 0.0% at nucleotide positions A12 and A18, respectively (fig. S6B). The other two candidate guides hEx52 sgRNA-2 and sgRNA-3 paired with ABEmax-SpCas9 were both relatively inefficient at the target A:T base pair (nucleotide position A12 editing of 2.3 ± 0.6% and nucleotide position A18 editing of 5.3 ± 0.6%, respectively) at the SAS AG sequence (fig. S6B).

Because of its high efficiency in inducing a single nucleotide transition at the SDS of exon 50, hEx50 sgRNA-1 was tested for its ability to promote exon skipping and restore dystrophin expression in human ΔEx51 iPSC–derived cardiomyocytes. Editing in ΔEx51 iPSCs with hEx50 sgRNA-1 and ABEmax-SpCas9 generated on-target editing at A14 of 87.7 ± 4.1%, with bystander editing at A18 of

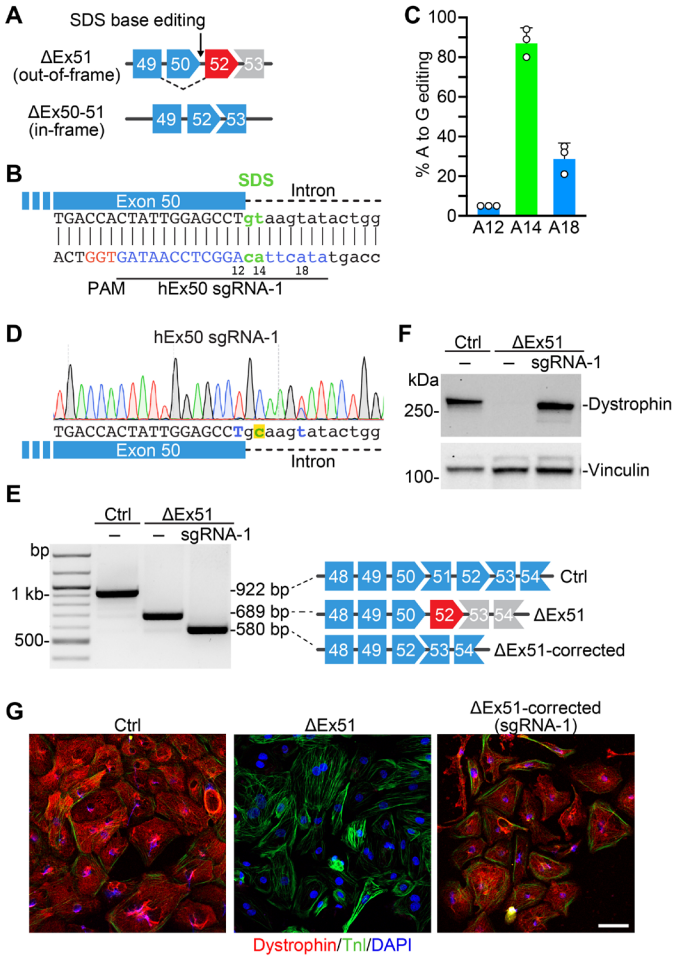

Fig. 4. Base editing–mediated exon skipping restores dystrophin expression in human ΔEx51 iPSC–derived cardiomyocytes. (**A**) Gene editing strategy to restore the in-frame ORF by exon skipping using base editing. (**B**) The hEx50 sgRNA-1 binding position in the region of the SDS of human *DMD* exon 50 (green). Sequence shows sgRNA (blue) and PAM (red). (**C**) Percentages of DNA editing of adenines in the editing window of ABEmax-SpCas9 with hEx50 sgRNA-1 following nucleofection in human ΔEx51 iPSCs. On-target edit (A14) is colored green. Dots and bars represent results of different nucleofections and are means ± SEM ($n = 3$). (**D**) Representative Sanger sequencing chromatogram of the genomic region of the exon 50 SDS of human iPSCs following nucleofection with ABEmax-SpCas9 and hEx50 sgRNA-1. (**E**) RT-PCR analysis of RNA from single clones of healthy control (Ctrl), ΔEx51, and corrected ΔEx51 iPSC–derived cardiomyocytes after base editing. (**F**) Western blot analysis of dystrophin protein expression of Ctrl, ΔEx51, and corrected ΔEx51 iPSC–derived cardiomyocytes. Vinculin is the loading control. (**G**) Immunocytochemistry of dystrophin in Ctrl, ΔEx51, and corrected ΔEx51 iPSC–derived cardiomyocytes. Dystrophin is indicated in red. Cardiac troponin-I (TnI) is indicated in green. Nuclei are marked by DAPI (4′,6-diamidino-2-phenylindole) (blue). Scale bar, 50 μm.

29.3 ± 4.3% and at A12 of 5.0 ± 0.0% (Fig. 4, C and D). As the bystander edits are located in the intron region or in the to-be-skipped exon, they are not predicted to affect the final dystrophin transcript.

Single clones of iPSCs containing a base-edited SDS GT dinucleotide sequence to a GC dinucleotide sequence were isolated and differentiated into cardiomyocytes. RT-PCR using primers that amplify the region from exon 48 to 54 and complementary DNA (cDNA) sequencing analysis showed skipping of exon 50 and splicing of exons 49 to 52 (Fig. 4E and fig. S6C).

Western blot analysis and immunocytochemistry showed restoration of dystrophin protein expression in ΔEx51 cardiomyocytes that had been corrected with hEx50 sgRNA-1 and ABEmax-SpCas9 (Fig. 4, F and G, and fig. S6D). These findings are consistent with previous studies on exon skipping correction strategies around the exon 50 to 51 locus in DMD patient–derived iPSC cardiomyocytes (*7*, *37*). Together, our data suggest that a single-swap transition generated by ABEmax at the SDS GT sequence of *DMD* exon 50 is sufficient to cause skipping of exon 50 in human DMD cells and restore dystrophin protein expression.

Prime editing of *DMD* exons can enable exon reframing and restore dystrophin expression in human cardiomyocytes

As we found base editing for exon 52 skipping to be relatively inefficient, we developed a prime editing–based reframing strategy for exon 52 as another potential gene editing correction strategy for the exon 51 deletion mutation in iPSC-derived cardiomyocytes (Fig. 5A). We reasoned that one of the keys to efficient prime editing is the efficiency of the sgRNA in the pegRNA construct. sgRNA efficiency prediction software using CRISPOR suggested that hEx52 sgRNA-4 was likely to be the most efficient sgRNA in exon 52 as calculated by scoring from Doench *et al.* (*38*), so we selected this sgRNA for further optimization in the pegRNA construct (fig. S7A). As prime editing allows discretionary gene insertions and deletions, we arbitrarily chose to introduce a +2-nt AC insertion at position +1 with respect to the nicking site generated by hEx52 sgRNA-4 (counting the PAM positions as +4 to +6). As hEx52 sgRNA-4 is in the antisense orientation and inserts the AC dinucleotide sequence on the antisense strand, the final *DMD* transcript will contain a GT dinucleotide insertion on the sense strand upon successful prime editing (Fig. 5B). Following recommendations for prime editing optimization (*22*), we started with a pegRNA with a PBS length of 13 nt and an RT template length of 15 nt (referred to as hEx52-PE) (Fig. 5B). We then systematically varied the lengths of the PBS and RT template to find the most highly efficient pegRNA. We found that while longer lengths of the PBS and RT template correlated with increased editing efficiency, the longest lengths performed comparably (fig. S7, B and C). To further optimize the editing efficiency, we also selected two nicking sgRNAs to pair with hEx52-PE, which cause a nick 29 nt upstream (nick-1, −29 nt) or a nick 52 nt downstream on the sense strand (nick-2, +52 nt) with respect to the nicking site generated by hEx52 sgRNA-4 (Fig. 5B).

We tested the efficiency of hEx52-PE in the ΔEx51 iPSC model with both nicking sgRNAs. We detected a 20.2% efficiency in introducing a +2-nt GT insertion on the sense strand at the desired position using hEx52-PE and nick-1 and a 54.0% efficiency using hEx52-PE and nick-2 (fig. S8A). We then differentiated the total mixture of edited and non-edited iPSCs into cardiomyocytes to determine the effects of the insertion on dystrophin recovery. The relative quantity of dystrophin protein with respect to the healthy control iPSC-derived cardiomyocytes was 24.8% after editing with hEx52-PE and nick-1 and 39.7% after editing with hEx52-PE and nick-2, which correlated with the DNA editing efficiencies (fig. S8, B and C).

Single clones of iPSCs with the prime-edited insertion in exon 52 were isolated and differentiated into cardiomyocytes. RT-PCR and cDNA sequencing analyses confirmed the precise GT insertion on the sense strand in exon 52 (Fig. 5, C and D). The correct reframing of the ORF was confirmed by the restoration of dystrophin protein

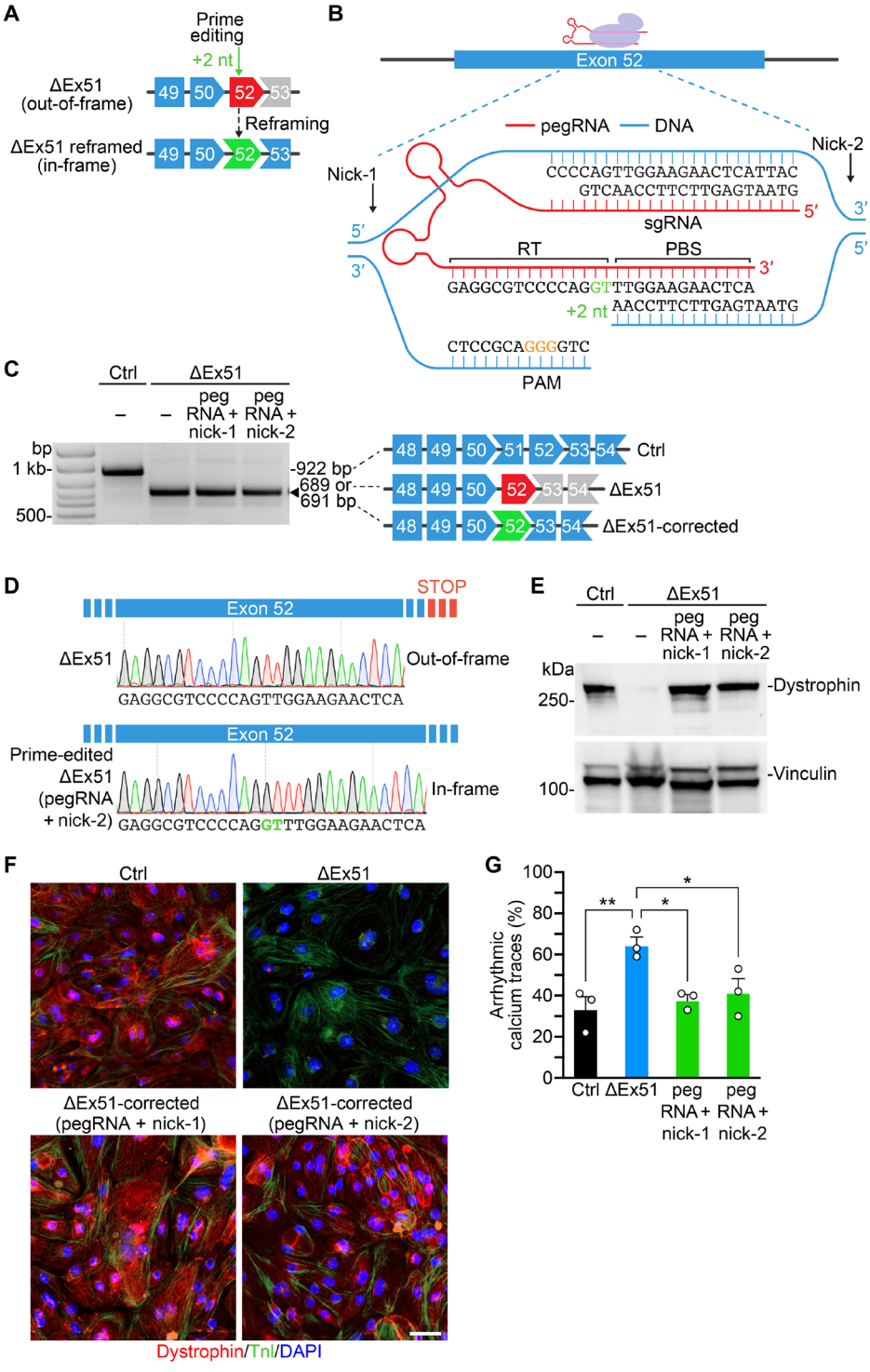

Fig. 5. Prime editing–mediated exon reframing restores dystrophin expression in human ΔEx51 iPSC–derived cardiomyocytes. (**A**) Gene editing strategy to restore the in-frame ORF by exon reframing using prime editing. (**B**) Illustration of the pegRNA used in the following experiments (red) and the target DNA sequence (blue). PAM is indicated in orange and programmed insertion in green. (**C**) RT-PCR analysis of RNA from single clones of healthy control (Ctrl), ΔEx51, and corrected ΔEx51 iPSC–derived cardiomyocytes after prime editing with nick-1 or nick-2. (**D**) Sanger sequencing chromatograms of the RT-PCR product of RNA from ΔEx51 iPSC–derived cardiomyocytes before and after prime editing. (**E**) Western blot analysis of dystrophin protein expression of Ctrl, ΔEx51, and corrected ΔEx51 iPSC–derived cardiomyocytes. Vinculin is the loading control. (**F**) Immunocytochemistry of dystrophin in Ctrl, ΔEx51, and corrected ΔEx51 iPSC–derived cardiomyocytes. Dystrophin is indicated in red. Cardiac troponin-I is indicated in green. Nuclei are marked by DAPI stain in blue. Scale bar, 50 μm. (**G**) Percentage of arrhythmic calcium traces of Ctrl, ΔEx51, and corrected ΔEx51 iPSC–derived cardiomyocytes. Dots and bars represent results of different biological replicates ($n = 216$ cells across three biological replicate experiments) and are means ± SEM ($n = 3$). *$P < 0.05$ and **$P < 0.001$ using unpaired two-tailed Student's t test.

expression, as demonstrated by Western blot analysis and immunocytochemistry (Fig. 5, E and F).

Prime editing of *DMD* exons normalizes contractile abnormalities of human DMD cardiomyocytes

We next investigated whether genome editing of cardiomyocytes by prime editing could rescue a possible arrhythmic defect in ΔEx51 cardiomyocytes. We treated 30-day-old iPSC-derived cardiomyocytes with isoproterenol and performed calcium-cycling analyses. We detected an arrhythmic defect in the ΔEx51 cardiomyocytes compared to the healthy control cardiomyocytes. This observation recapitulates patient phenotypes (*39*) and human cardiac iPSC models of DMD (*5*, *40*), with a significant increase in the percentage of arrhythmic calcium traces from 33.7 ± 5.6% of the healthy control cardiomyocytes to 64.7 ± 3.8% of ΔEx51 cardiomyocytes (Fig. 5G and fig. S8, D and E). Our observation that a fraction of ΔEx51 cardiomyocytes did not exhibit an arrhythmic phenotype could stem from the transcriptional, structural, and functional heterogeneity of iPSC-derived cardiomyocytes (*41*, *42*), whereby cardiomyocytes from different lineages (i.e., nodal, atrial, and ventricular) could display variable susceptibilities to arrhythmias. A similar observation was reported in other studies investigating the electrophysiological properties of iPSC-derived cardiomyocytes in the setting of diseases that affect cardiac electrophysiology (*40*, *43*, *44*). In contrast, prime-edited ΔEx51 cardiomyocytes exhibited a percentage of arrhythmic calcium traces comparable to that of the healthy control cardiomyocytes (38.0 ± 2.5% after editing with hEx52-PE and nick-1 and 41.7 ± 6.6% after editing with hEx52-PE and nick-2), confirming alleviation of the arrhythmic defect in prime-edited–reframed ΔEx51 cardiomyocytes (Fig. 5G and fig. S8D). Together, these data demonstrate that prime editing can be used to precisely reframe the correct ORF and restore functional dystrophin expression in cultured human ΔEx51 iPSC cardiomyocytes when cells are nucleofected and sorted to isolate transfected cells.

DISCUSSION

Our results demonstrate the effectiveness of two different nucleotide genome editing techniques, base editing and prime editing, for the correction of one of the most common single-exon mutations in patients with *DMD* deletion of exon 51 in the dystrophin gene (*23*). Our laboratory and others previously demonstrated the efficacy of in vivo gene editing to correct DMD-causing mutations by the introduction of INDELs within or surrounding out-of-frame exons using CRISPR-Cas9 (*4*, *6*, *8*, *9*, *34*, *45*–*47*). One approach to restore the correct ORF in mutated dystrophin transcripts, referred to as double-cut myoediting, used CRISPR-Cas9 and a pair of sgRNAs to introduce two cuts in the DNA to remove intervening target exons for exon skipping. However, double-cut myoediting in its current iterations has limitations in its therapeutic applicability because of its low editing efficiency and its generation of unpredictable genome modifications, such as AAV integration and DNA inversion (*34*). Another genome editing approach, single-cut myoediting, overcomes some of these limitations by using CRISPR-Cas9 and one sgRNA to introduce one cut in the DNA in the proximity of splice sites to cause exon skipping following small deletions or exon reframing following insertion or deletion of appropriate numbers of nucleotides within out-of-frame exons (*4*). However, both double- and single-cut myoediting rely on the generation of DSBs in the genome and the NHEJ repair pathway to introduce random INDELs at the cutting site.

Here, we investigated the use of nucleotide editing, namely base editing or prime editing, to induce exon skipping or exon reframing, respectively, to correct the *DMD* exon 51 deletion mutation. These two technologies do not introduce DSBs in the genome and offer more precision in the final editing outcome as they do not rely on random INDEL generation for gene editing. However, these advantages are tempered by the size of these nucleotide editing systems, as they both exceed the current packaging size limitation of AAV.

We demonstrated that ABEmax-SpCas9-NG can be delivered in vivo in a mouse model as a split-intein dual-AAV system and correct the ΔEx51 mutation in postmitotic skeletal muscle. We used SpCas9-NG because of its more relaxed NG PAM requirement compared to other Cas nucleases with more stringent PAM requirements (*48*). This increases the number of available sgRNAs that are positioned to edit SAS or SDS. We selected ABEmax as base editor as it is associated with fewer off-target consequences compared to CBEs (*18*–*21*). We found that intramuscular delivery of the split-intein dual-AAV system edits the SDS of exon 50 in muscles of the ΔEx51 mouse model.

Correction of DMD mutations by base editing of splice sites

The single swap of a nucleotide base pair in the GT SDS consensus sequence was sufficient to induce exon skipping and restore production of an internally deleted but functional dystrophin protein. Deletion of exon 51 eliminates 78 amino acids from the highly redundant central rod domain of dystrophin. Skipping of exon 50 to enable splicing of exons 49 to 52 restores the ORF of dystrophin. Because exon 50 encodes only 36 amino acids in the central rod domain, the corrected form of the dystrophin protein contains 97% of the 3685 amino acids of the full-length dystrophin protein and is therefore expected to be highly functional. In contrast, "micro-dystrophins" currently used in DMD gene therapy clinical trials contain approximately 30% of the dystrophin protein and are relatively functionally compromised.

One of the potential concerns reported for base editors is off-target editing. Our off-target analysis did not detect any notable off-target edits in the tested sites. Base editors, such as ABEmax, can edit all available base pairs within a defined activity window. These bystander edits can potentially be disadvantageous in some gene editing applications. For exon skipping, however, bystander edits would occur in the intron or in the to-be-skipped exon and thus not affect the final dystrophin transcript, which makes it an attractive gene editing strategy for correction of DMD mutations.

Adenine base editing as a gene therapy has been previously demonstrated in an adult mouse model of DMD harboring a nonsense point mutation in exon 20. Intramuscular injection of dual trans-splicing viral vectors containing the split ABE and one copy of sgRNA into the TA muscle of these DMD mice resulted in restoration of dystrophin expression in a modest percentage of myofibers (*15*). Their findings of lower dystrophin expression could be due to differences in the editing efficiency of the sgRNA, the ABE system, the age of the injected mice, or the splicing strategy. Their study used a trans-splicing dual-AAV strategy, which has been shown to have relatively poor transduction efficiency of the packaged transgene compared to single-vector or split-intein AAV systems, which limits its therapeutic potential (*49*). This is likely due to

the need for trans-splicing AAVs to undergo complex intermolecular concatamerization/recombination and subsequent splicing between the two vectors to reconstitute gene expression (*50*). We used a split-intein dual-AAV system that reconstitutes the full-length base editor by protein trans-splicing and has been previously shown to be as efficient as a full-length non–split-intein base editor (*29*). That study also demonstrated correction of a nonsense mutation (p.Q871X) for which the human equivalent mutation (p.Q869X) has been clinically documented in only a few patients. Furthermore, nonsense mutations make up only 10% of the more than 7000 documented DMD-causing mutations and are evenly distributed across all 79 exons of the largest human gene. On the other hand, exon deletion mutations cluster in a hotspot region of the *DMD* gene and account for 68% of all total mutations with deletion of exon 51 being the second most common single-exon deletion mutation. Correction strategies for skipping of exon 50 would benefit not only the single exon 51 deletion mutation but also some multi-exon deletion mutations and could be therapeutically applicable to 4% of all patients with DMD (*2*, *51*).

To evaluate the clinical applicability of base editing, we also demonstrated that the single-swap strategy restores dystrophin expression in human iPSCs with deletion of exon 51 in the *DMD* gene. Base editing was originally envisioned to correct disease-causing point mutations in the genome; however, its utility in inducing exon skipping has become increasingly more intriguing because of its more flexible applications as a gene correction strategy (*16*). In this work, we used ABEmax as a base editor for exon skipping; however, other groups also have demonstrated the use of a cytidine deaminase base editor for exon skipping (*17*). In the future, the continuous optimization of more efficient base editors will further increase the efficiency of single-swap–based exon skipping using base editors. For exon skipping, the destruction of a splice site can activate new cryptic splice sites around that exon. This potential for alternative splicing and failure of exon skipping necessitates the need to determine or predict splicing outcomes after base editing.

Correction of disease-causing mutations by reframing through prime editing

While base editing at the exon 52 SAS for exon skipping was relatively inefficient in our initial screen, we found that prime editing generated a desired +2-nt insertion within exon 52 for exon reframing and serves as an additional nucleotide editing strategy. While INDEL profiles from CRISPR-induced DSBs may have some sequence-dependent predictability in INDEL outcomes (*52*), the INDEL profiles are nonetheless heterogeneous in their outcome and are site specific. NHEJ-based INDEL correction thus may produce both nonproductive edits and productive edits in restoring the ORF. Prime editing has an advantage of specifying the exact insertion or deletion outcome for exon reframing, thereby ensuring that all of the edits are productive in restoring the correct ORF. Furthermore, in NHEJ-based INDEL correction, a nonproductive edit prevents the sgRNA from reannealing to the site and inducing a productive edit. In prime editing, a nonproductive event (i.e., no editing as the edited strand is not successfully incorporated, leaving the native sequence intact) leaves the sgRNA target site still amenable to reannealing and another attempt at inducing the desired edit.

Our demonstration that prime editing can correct DMD-causing mutations opens interesting new possibilities. First, prime editing can theoretically be used to correct all possible point mutations including base pair transitions and transversions, whereas base editors are limited only to transitions of A:T to G:C or C:G to T:A. In addition, as shown here, the correction of exon deletion mutations by precise exon reframing instead of exon skipping allows retention of the edited exon, therefore minimizing the number of amino acids that are missing from the final dystrophin protein. As prime editing necessitates the coordination of multiple pegRNA components for editing, such as the spacer sequence, the PBS, and the RT template, it is likely that editing events at off-target sites are minimal. However, a recent preprint demonstrated that two opposite strand nicks using the PE3 system can cause undesired editing outcomes in mouse zygote injections (*53*). These undesired editing outcomes were reduced by using an sgRNA that is mutation specific and can nick only after successful editing and resolution of the pegRNA nick (PE3b system). All of these limitations, together with the large size of the prime editing construct that precludes single-vector AAV packaging, have to be taken into consideration before moving to in vivo genome editing by prime editing.

Looking to the future

Future studies will need to address several remaining questions concerning nucleotide editing as a therapeutic strategy for DMD. While we have shown dystrophin restoration in a mouse model using a split-intein dual-AAV system, clinical translation of our work is still far, and it would need to be demonstrated in large animal models and evaluated for efficacy and safety. The high editing efficiency that we detected in vivo is evidently influenced by the elevated viral dose that we used. We injected in the TA (average weight of ~6.5 mg) of P12 ΔEx51 mouse a 1×10^{11} vg/kg dose, which corresponds to a theoretically equivalent systemic dose of ~1.5×10^{16} vg/kg. This is much greater than the highest systemic AAV9 dose currently permitted (3×10^{14}) by the U.S. Food and Drug Administration. In addition, as transduction efficiency in immature myofibers of P12 mice is likely higher than in mature myofibers, which are surrounded by more connective tissue and extracellular matrix, the editing efficiency in older mice should be analyzed in the future.

Long-term studies will need to be performed to determine the longevity of rescue, potential consequences of persistent in vivo expression of base editors or prime editors, and the potential contribution of muscle satellite cells to gene-edited skeletal muscle following muscle repair and regeneration. In this regard, recent work demonstrated that the AAV9 serotype and CK8e promoter can transduce and deliver editing systems to muscle satellite cells and drive expression of the packaged transgene (*54*, *55*). However, further studies to determine the minimal viral dose for satellite cell transduction and the most efficient promoters for expression of gene editing components need to be performed before clinical translation of skeletal muscle gene editing. Questions about possible immunological responses to base editors or prime editors have also not been addressed.

Nucleotide editing technologies have the potential to eliminate disease-causing mutations following a single treatment. Here, we demonstrate a unique utilization of these two technologies as a gene therapy strategy to induce exon skipping or reframing in an exon deletion DMD model. These new editing tools and strategies complement previous genome editing approaches developed for the correction of DMD and represent a step toward clinical correction of DMD and other genetic neuromuscular disorders.

MATERIALS AND METHODS

Study design

This study aimed to use nucleotide editing technologies to correct the DMD-causing ΔEx51 deletion mutation in the *DMD* gene in both a mouse model and a human iPSC model of DMD. This resulted in rescue of dystrophin protein expression, improvement of skeletal muscle fiber architecture in vivo, and reduction of arrhythmic cardiomyocytes in human iPSCs. We tested in vitro mouse sgRNAs for base editing that target SAS or SDS of exon 50 or 52, and we evaluated genome editing efficiencies using Sanger sequencing. We used AAV9 to deliver, in vivo, the sgRNA with the highest efficiency and an ABE by intramuscular injection. We evaluated the editing outcomes using Sanger sequencing, RT-PCR, Western blot analysis, immunohistochemistry, and H&E staining. Mice injected with saline solution served as a control. As an additional control, one leg of the mouse was injected with saline solution and the other leg with AAV containing the base editing components. We tested in vitro human sgRNAs for gene correction by base editing or prime editing. The optimal sgRNAs were nucleofected into iPSCs with the ΔEx51 mutation. Editing outcomes were evaluated in iPSC-derived cardiomyocytes by Sanger sequencing, RT-PCR, Western blot analysis, immunocytochemistry, and calcium imaging. Each experiment was conducted in replicate as indicated by *n* values in the figure legends. Sample size was chosen to use the fewest number of animals to achieve statistical significance; no statistical methods were used to predetermine sample size. All experimental samples were included in the analyses, with no data excluded.

Study approval

All experimental procedures involving animals in this study were reviewed and approved by the University of Texas Southwestern Medical Center's Institutional Animal Care and Use Committee.

Plasmids and cloning

The pmCherry_gRNA plasmid contained a U6-driven sgRNA scaffold and a cytomegalovirus (CMV)–driven pmCherry fluorescent protein. pmCherry_gRNA was a gift from E. Welker (Addgene plasmid #80457). pCMV_ABEmax_P2A_GFP (Addgene plasmid #112101) (*24*), NG-ABEmax (Addgene plasmid #124163) (*28*), pCMV-PE2-P2A-GFP (Addgene plasmid #132776) (*22*), and pU6-pegRNA-GG-acceptor (Addgene plasmid #132777) (*22*) were gifts from D. Liu. The N-terminal ABE and C-terminal ABE constructs were adapted from Cbh_v5 AAV-ABE N terminus (Addgene plasmid #137177) (*29*) and Cbh_v5 AAV-ABE C terminus (Addgene plasmid #137178) (*29*) and synthesized by Twist Bioscience and GenScript. The pSpCas9(BB)-2A-GFP (PX458) plasmid used for the generation of isogenic ΔEx51 iPSCs was a gift from F. Zhang (Addgene plasmid #48138) (*56*). Cloning of sgRNAs was done using NEBuilder HiFi DNA Assembly (NEB) into restriction enzyme–digested destination vectors.

Cell culture and transfection

N2a and 293T cells were maintained in Dulbecco's modified Eagle's medium supplemented with 10% (v/v) fetal bovine serum. For transfection experiments, cells were seeded onto 24-well plates at 125,000 cells per well. The following day, cells were transfected by Lipofectamine 2000 (Thermo Fisher Scientific), according to the manufacturer's instructions. Cells were harvested for downstream analyses 3 days later. The sequences of the tested sgRNAs are listed in table S1.

Sequencing analysis

Genomic DNA of mouse N2a cells, human 293T cells, and human iPSCs was isolated using DirectPCR cell lysis reagent (Viagen) supplemented with proteinase K (1 μg/μl) according to the manufacturer's protocol. Genomic DNA of mouse muscle tissues was isolated using the DNeasy Blood and Tissue Kit (Qiagen) according to the manufacturer's protocol. Total RNA of mouse skeletal muscles and human iPSC-derived cardiomyocytes was isolated using RNeasy Mini Kit (Qiagen) according to the manufacturer's protocol. cDNA was reverse-transcribed from total RNA using the iScript cDNA Synthesis Kit (Bio-Rad Laboratories). Genomic DNA and cDNA were PCR-amplified using PrimeSTAR GXL DNA polymerase (Takara). The top eight potential off-target sites were predicted by CRISPOR (*32*). Base editing on-target and off-target efficiencies were analyzed from Sanger sequencing by EditR (*57*). Prime editing efficiency was analyzed from Sanger sequencing by TIDE analysis (*58*). Primers of the PCR reactions are listed in table S1.

AAV vector production

AAVs were prepared by the Boston Children's Hospital Viral Core, as previously described (*58*). AAV vectors were purified by discontinuous iodixanol gradients (Cosmo Bio, AXS-1114542-5) and concentrated with a Millipore Amicon filter unit (UFC910008, 100 kDa). AAV titers were determined by quantitative real-time PCR assays.

Mice

Mice were housed in a barrier facility with a 12-hour:12-hour light:dark cycle and maintained on standard chow (2916 Teklad Global). ΔEx51 mice and WT littermates were genotyped as previously described (*26*). All experiments used only male mice. Animals were assigned to experimental groups by genotype. We did not use exclusion, randomization, or blinding approaches to assign animals for experiments. All AAV injections and dissections were conducted in an unblinded fashion.

AAV9 delivery to ΔEx51 mice

Before intramuscular injections, mice were anesthetized by intraperitoneal injection of a ketamine and xylazine anesthetic cocktail. Intramuscular injection of P12 male ΔEx51 mice was performed via slow longitudinal injection into TA muscles using an ultrafine needle (31 gauge) with 50 μl of saline solution or a prepared mixture of the dual-AAV9 viruses (5×10^{10} vg per leg of each virus).

Western blot analysis

Western blot analyses were performed as previously described (*9*). Briefly, for Western blots of muscles, tissues were crushed using a liquid nitrogen–frozen crushing apparatus. For Western blots of iPSC-derived cardiomyocytes, 2×10^6 cardiomyocytes were harvested and lysed in lysis buffer [10% sodium dodecyl sulfate, 62.5 mM tris (pH 6.8), 1 mM EDTA, and protease inhibitor] with a pestle. Cell or tissue lysates were passed through a 25-gauge syringe and then a 27-gauge syringe, 10 times each. Fifty micrograms of total protein was loaded onto a 4 to 20% acrylamide gel. Blots were then incubated with mouse anti-dystrophin antibody (Sigma-Aldrich, D8168) at 4°C overnight for dystrophin detection or with anti-vinculin antibody (Sigma-Aldrich, V9131) at room temperature for 1 hour for vinculin detection (loading control) and then with horseradish peroxidase antibody (Bio-Rad Laboratories) at room temperature for 1 hour. Blots were developed using Western blotting luminol reagent (Santa Cruz Biotechnology, sc-2048).

Histological analyses of skeletal muscles

Muscles were individually dissected and cryo-embedded in a 1:2 volume mixture of Gum Tragacanth powder (Sigma-Aldrich) to tissue freezing medium (Triangle Bioscience). All embeds were snap-frozen in isopentane heat extractant and supercooled to −155°C. Eight-micrometer transverse sections of muscle were prepared on a Leica CM3050 cryostat. H&E staining was performed as previously described in established staining protocols (*45*). Dystrophin immunohistochemistry was performed using MANDYS8 monoclonal antibody (Sigma-Aldrich, D8168) with modifications to the manufacturer's instructions as previously described (*9*). Image analyses were performed using Fiji software (*59*) on at least three muscles for each condition as indicated in the figures. Myofiber diameter was calculated as minimal Feret's diameter, a geometrical parameter for reliable measurement of cross-sectional size (*60*).

Human iPSC maintenance and nucleofection

Human iPSCs were cultured on Matrigel-coated polystyrene tissue culture plates and maintained in mTeSR Plus media (Stem Cell Technologies). Cells were passaged at 60 to 80% confluence using Versene (Gibco). One hour before nucleofection, iPSCs were treated with 10 μM ROCK inhibitor, Y-27632 (Selleckchem). iPSCs were then dissociated into single cells using Accutase (Innovative Cell Technologies). For the base editing studies, iPSCs (8×10^5) were mixed with 1.5 μg of pmCherry_gRNA plasmid containing the target sgRNA and 4.5 μg of pCMV_ABEmax_P2A_GFP. For the prime editing studies, iPSCs (8×10^5) were mixed with 500 ng of pmCherry_gRNA plasmid containing the nicking sgRNA, 1.5 μg of the pU6-pegRNA-GG-acceptor plasmid containing the target pegRNA, and 4.5 μg of the pCMV-PE2-P2A-GFP plasmid. iPSCs were then nucleofected using the P3 Primary Cell 4D-Nucleofector X Kit (Lonza) according to the manufacturer's protocol. After nucleofection, iPSCs were cultured in mTeSR Plus media supplemented with 10 μM ROCK inhibitor and Primocin (100 μg/ml) (InvivoGen) and then switched to fresh mTeSR Plus media the following day. Three days after nucleofection, green fluorescent protein (GFP) and pmCherry double-positive cells were isolated by fluorescence-activated cell sorting. Mixed population or single clones were isolated, expanded, genotyped, and sequenced.

Human iPSC cardiomyocyte differentiation

Human iPSCs at 60 to 80% confluency were differentiated into cardiomyocytes as previously described (*61*). Briefly, cells were cultured in CDM3 media supplemented with 4 to 6 μM CHIR99021 (Selleckchem) for 48 hours (days 1 to 2) and then CDM3 media supplemented with 2 μM WNT-C59 (Selleckchem) for 48 hours (days 3 to 4). Starting on day 5, cells were cultured in basal media [RPMI 1640 (Gibco) supplemented with B-27 supplement (Thermo Fisher Scientific)] for 6 days (days 5 to 10). On day 10, cells were cultured in selective media [RPMI 1640, without glucose (Gibco), supplemented with B-27 supplement] for 10 days (days 11 to 20) and then basal media thereafter. Cardiomyocytes were used for experiments on day 30 and harvested using TrypLE Express (Thermo Fisher Scientific).

Human iPSC cardiomyocyte immunocytochemistry

Dystrophin and troponin-I immunocytochemistry of iPSC-derived cardiomyocytes was performed as previously described (*5*). Briefly, iPSC-derived cardiomyocytes (1×10^5) were seeded on 12-mm coverslips coated with poly-D-lysine and Matrigel (Corning) and fixed in cold acetone (10 min, −20°C). Following fixation, coverslips were equilibrated in phosphate-buffered saline and then blocked for 1 hour with serum cocktail [2% normal horse serum/2% normal donkey serum/0.2% bovine serum albumin (BSA)/phosphate-buffered saline]. Mouse anti-dystrophin (1:800) (MANDYS8, Sigma-Aldrich, D8168) and rabbit anti–troponin-I (1:200) (clone H170, Santa Cruz Biotechnology, sc-15368) in 0.2% BSA/phosphate-buffered saline were applied and incubated overnight at 4°C. Then, coverslips were probed for 1 hour with biotinylated horse anti-mouse immunoglobulin G (IgG) (1:200) (Vector Laboratories, BA-2000) and fluorescein-conjugated donkey anti-rabbit IgG (1:50) (Jackson ImmunoResearch, 711-095-152) diluted in 0.2% BSA/phosphate-buffered saline. Unbound secondary antibodies were removed with phosphate-buffered saline washes, and final dystrophin labeling was done with a 10-min incubation of rhodamine avidin DCS (1:60) (Vector Laboratories) diluted in phosphate-buffered saline.

Human iPSC cardiomyocyte calcium imaging

Calcium imaging of human iPSC-derived cardiomyocytes was performed as previously described (*41*). Beating cardiomyocytes were dissociated into a single-cell suspension and seeded on a glass-bottom dish at single-cell density. Cells were loaded with the fluorescent calcium indicator Fluo-4 AM (Thermo Fisher Scientific) at 2 μM for 30 min and then cultured in medium containing 0 or 10 μM isoproterenol (Sigma-Aldrich) for another 30 min before imaging. Spontaneous Ca^{2+} transients of beating iPSC-derived cardiomyocytes were imaged at 37°C using a Nikon A1R+ confocal system. Ca^{2+} transients were processed using Fiji software (*59*) and analyzed using Microsoft Excel.

Statistics

All data are presented as means ± SEM. Unpaired two-tailed Student's *t* tests were performed for comparison between the respective two groups as indicated in the figures. Data analyses were performed with statistical software (GraphPad Prism Software). *P* values less than 0.05 were considered statistically significant.

SUPPLEMENTARY MATERIALS

Supplementary material for this article is available at http://advances.sciencemag.org/cgi/content/full/7/18/eabg4910/DC1

View/request a protocol for this paper from *Bio-protocol*.

REFERENCES AND NOTES

1. E. P. Hoffman, R. H. Brown Jr., L. M. Kunkel, Dystrophin: The protein product of the duchenne muscular-dystrophy locus. *Cell* **51**, 919–928 (1987).
2. K. M. Flanigan, D. M. Dunn, A. von Niederhausern, P. Soltanzadeh, E. Gappmaier, M. T. Howard, J. B. Sampson, J. R. Mendell, C. Wall, W. M. King, A. Pestronk, J. M. Florence, A. M. Connolly, K. D. Mathews, C. M. Stephan, K. S. Laubenthal, B. L. Wong, P. J. Morehart, A. Meyer, R. S. Finkel, C. G. Bonnemann, L. Medne, J. W. Day, J. C. Dalton, M. K. Margolis, V. J. Hinton; United Dystrophinopathy Project Consortium, R. B. Weiss, Mutational spectrum of DMD mutations in dystrophinopathy patients: Application of modern diagnostic techniques to a large cohort. *Hum. Mutat.* **30**, 1657–1666 (2009).
3. F. Muntoni, S. Torelli, A. Ferlini, Dystrophin and mutations: One gene, several proteins, multiple phenotypes. *Lancet Neurol.* **2**, 731–740 (2003).
4. L. Amoasii, C. Long, H. Li, A. A. Mireault, J. M. Shelton, E. Sanchez-Ortiz, J. R. McAnally, S. Bhattacharyya, F. Schmidt, D. Grimm, S. D. Hauschka, R. Bassel-Duby, E. N. Olson, Single-cut genome editing restores dystrophin expression in a new mouse model of muscular dystrophy. *Sci. Transl. Med.* **9**, eaan8081 (2017).
5. V. Kyrychenko, S. Kyrychenko, M. Tiburcy, J. M. Shelton, C. Long, J. W. Schneider, W.-H. Zimmermann, R. Bassel-Duby, E. N. Olson, Functional correction of dystrophin actin binding domain mutations by genome editing. *JCI Insight* **2**, e95918 (2017).

6. L. Amoasii, J. C. W. Hildyard, H. Li, E. Sanchez-Ortiz, A. Mireault, D. Caballero, R. Harron, T. R. Stathopoulou, C. Massey, J. M. Shelton, R. Bassel-Duby, R. J. Piercy, E. N. Olson, Gene editing restores dystrophin expression in a canine model of Duchenne muscular dystrophy. *Science* **362**, 86–91 (2018).
7. C. Long, H. Li, M. Tiburcy, C. Rodriguez-Caycedo, V. Kyrychenko, H. Zhou, Y. Zhang, Y.-L. Min, J. M. Shelton, P. P. A. Mammen, N. Y. Liaw, W.-H. Zimmermann, R. Bassel-Duby, J. W. Schneider, E. N. Olson, Correction of diverse muscular dystrophy mutations in human engineered heart muscle by single-site genome editing. *Sci. Adv.* **4**, eaap9004 (2018).
8. Y.-L. Min, H. Li, C. Rodriguez-Caycedo, A. A. Mireault, J. Huang, J. M. Shelton, J. R. McAnally, L. Amoasii, P. P. A. Mammen, R. Bassel-Duby, E. N. Olson, CRISPR-Cas9 corrects Duchenne muscular dystrophy exon 44 deletion mutations in mice and human cells. *Sci. Adv.* **5**, eaav4324 (2019).
9. Y. L. Min, F. Chemello, H. Li, C. Rodriguez-Caycedo, E. Sanchez-Ortiz, A. A. Mireault, J. R. McAnally, J. M. Shelton, Y. Zhang, R. Bassel-Duby, E. N. Olson, Correction of three prominent mutations in mouse and human models of duchenne muscular dystrophy by single-cut genome editing. *Mol. Ther.* **28**, 2044–2055 (2020).
10. A. Moretti, L. Fonteyne, F. Giesert, P. Hoppmann, A. B. Meier, T. Bozoglu, A. Baehr, C. M. Schneider, D. Sinnecker, K. Klett, T. Fröhlich, F. A. Rahman, T. Haufe, S. Sun, V. Jurisch, B. Kessler, R. Hinkel, R. Dirschinger, E. Martens, C. Jilek, A. Graf, S. Krebs, G. Santamaria, M. Kurome, V. Zakhartchenko, B. Campbell, K. Voelse, A. Wolf, T. Ziegler, S. Reichert, S. Lee, F. Flenkenthaler, T. Dorn, I. Jeremias, H. Blum, A. Dendorfer, A. Schnieke, S. Krause, M. C. Walter, N. Klymiuk, K. L. Laugwitz, E. Wolf, W. Wurst, C. Kupatt, Somatic gene editing ameliorates skeletal and cardiac muscle failure in pig and human models of Duchenne muscular dystrophy. *Nat. Med.* **26**, 207–214 (2020).
11. Y. L. Min, R. Bassel-Duby, E. N. Olson, CRISPR correction of Duchenne muscular dystrophy. *Annu. Rev. Med.* **70**, 239–255 (2019).
12. F. Chemello, R. Bassel-Duby, E. N. Olson, Correction of muscular dystrophies by CRISPR gene editing. *J. Clin. Invest.* **130**, 2766–2776 (2020).
13. H. A. Rees, D. R. Liu, Base editing: Precision chemistry on the genome and transcriptome of living cells. *Nat. Rev. Genet.* **19**, 770–788 (2018).
14. K. Kim, S. M. Ryu, S. T. Kim, G. Baek, D. Kim, K. Lim, E. Chung, S. Kim, J. S. Kim, Highly efficient RNA-guided base editing in mouse embryos. *Nat. Biotechnol.* **35**, 435–437 (2017).
15. S. M. Ryu, T. Koo, K. Kim, K. Lim, G. Baek, S. T. Kim, H. S. Kim, D. E. Kim, H. Lee, E. Chung, J. S. Kim, Adenine base editing in mouse embryos and an adult mouse model of Duchenne muscular dystrophy. *Nat. Biotechnol.* **36**, 536–539 (2018).
16. M. Gapinske, A. Luu, J. Winter, W. S. Woods, K. A. Kostan, N. Shiva, J. S. Song, P. Perez-Pinera, CRISPR-SKIP: Programmable gene splicing with single base editors. *Genome Biol.* **19**, 107 (2018).
17. J. Yuan, Y. Ma, T. Huang, Y. Chen, Y. Peng, B. Li, J. Li, Y. Zhang, B. Song, X. Sun, Q. Ding, Y. Song, X. Chang, Genetic modulation of RNA splicing with a CRISPR-guided cytidine deaminase. *Mol. Cell* **72**, 380–394.e7 (2018).
18. J. Grunewald, R. Zhou, S. P. Garcia, S. Iyer, C. A. Lareau, M. J. Aryee, J. K. Joung, Transcriptome-wide off-target RNA editing induced by CRISPR-guided DNA base editors. *Nature* **569**, 433–437 (2019).
19. S. Jin, Y. Zong, Q. Gao, Z. Zhu, Y. Wang, P. Qin, C. Liang, D. Wang, J.-L. Qiu, F. Zhang, C. Gao, Cytosine, but not adenine, base editors induce genome-wide off-target mutations in rice. *Science* **364**, 292–295 (2019).
20. E. Zuo, Y. Sun, W. Wei, T. Yuan, W. Ying, H. Sun, L. Yuan, L. M. Steinmetz, Y. Li, H. Yang, Cytosine base editor generates substantial off-target single-nucleotide variants in mouse embryos. *Science* **364**, 289–292 (2019).
21. H. K. Lee, H. E. Smith, C. Liu, M. Willi, L. Hennighausen, Cytosine base editor 4 but not adenine base editor generates off-target mutations in mouse embryos. *Commun. Biol.* **3**, 19 (2020).
22. A. V. Anzalone, P. B. Randolph, J. R. Davis, A. A. Sousa, L. W. Koblan, J. M. Levy, P. J. Chen, C. Wilson, G. A. Newby, A. Raguram, D. R. Liu, Search-and-replace genome editing without double-strand breaks or donor DNA. *Nature* **576**, 149–157 (2019).
23. Y. Echigoya, K. R. Q. Lim, A. Nakamura, T. Yokota, Multiple exon skipping in the Duchenne muscular dystrophy hot spots: Prospects and challenges. *J. Pers. Med.* **8**, 41 (2018).
24. L. W. Koblan, J. L. Doman, C. Wilson, J. M. Levy, T. Tay, G. A. Newby, J. P. Maianti, A. Raguram, D. R. Liu, Improving cytidine and adenine base editors by expression optimization and ancestral reconstruction. *Nat. Biotechnol.* **36**, 843–846 (2018).
25. A. Aartsma-Rus, I. Fokkema, J. Verschuuren, I. Ginjaar, J. van Deutekom, G. J. van Ommen, J. T. den Dunnen, Theoretic applicability of antisense-mediated exon skipping for Duchenne muscular dystrophy mutations. *Hum. Mutat.* **30**, 293–299 (2009).
26. F. Chemello, Z. Wang, H. Li, J. R. McAnally, N. Liu, R. Bassel-Duby, E. N. Olson, Degenerative and regenerative pathways underlying Duchenne muscular dystrophy revealed by single-nucleus RNA sequencing. *Proc. Natl. Acad. Sci. U.S.A.* **117**, 29691–29701 (2020).
27. S. M. Berget, Exon recognition in vertebrate splicing. *J. Biol. Chem.* **270**, 2411–2414 (1995).
28. T. P. Huang, K. T. Zhao, S. M. Miller, N. M. Gaudelli, B. L. Oakes, C. Fellmann, D. F. Savage, D. R. Liu, Circularly permuted and PAM-modified Cas9 variants broaden the targeting scope of base editors. *Nat. Biotechnol.* **37**, 626–631 (2019).
29. J. M. Levy, W. H. Yeh, N. Pendse, J. R. Davis, E. Hennessey, R. Butcher, L. W. Koblan, J. Comander, Q. Liu, D. R. Liu, Cytosine and adenine base editing of the brain, liver, retina, heart and skeletal muscle of mice via adeno-associated viruses. *Nat. Biomed. Eng.* **4**, 97–110 (2020).
30. M. Martari, A. Sagazio, A. Mohamadi, Q. Nguyen, S. D. Hauschka, E. Kim, R. Salvatori, Partial rescue of growth failure in growth hormone (GH)-deficient mice by a single injection of a double-stranded adeno-associated viral vector expressing the GH gene driven by a muscle-specific regulatory cassette. *Hum. Gene Ther.* **20**, 759–766 (2009).
31. J.-H. Choi, N.-K. Yu, G.-C. Baek, J. Bakes, D. Seo, H. J. Nam, S. H. Baek, C.-S. Lim, Y.-S. Lee, B.-K. Kaang, Optimization of AAV expression cassettes to improve packaging capacity and transgene expression in neurons. *Mol. Brain* **7**, 17 (2014).
32. J. P. Concordet, M. Haeussler, CRISPOR: Intuitive guide selection for CRISPR/Cas9 genome editing experiments and screens. *Nucleic Acids Res.* **46**, W242–W245 (2018).
33. C. H. Hakim, N. B. Wasala, C. E. Nelson, L. P. Wasala, Y. Yue, J. A. Louderman, T. B. Lessa, A. Dai, K. Zhang, G. J. Jenkins, M. E. Nance, X. Pan, K. Kodippili, N. N. Yang, S. J. Chen, C. A. Gersbach, D. Duan, AAV CRISPR editing rescues cardiac and muscle function for 18 months in dystrophic mice. *JCI Insight* **3**, e124297 (2018).
34. C. E. Nelson, Y. Wu, M. P. Gemberling, M. L. Oliver, M. A. Waller, J. D. Bohning, J. N. Robinson-Hamm, K. Bulaklak, R. M. Castellanos Rivera, J. H. Collier, A. Asokan, C. A. Gersbach, Long-term evaluation of AAV-CRISPR genome editing for Duchenne muscular dystrophy. *Nat. Med.* **25**, 427–432 (2019).
35. C. Bock, E. Kiskinis, G. Verstappen, H. Gu, G. Boulting, Z. D. Smith, M. Ziller, G. F. Croft, M. W. Amoroso, D. H. Oakley, A. Gnirke, K. Eggan, A. Meissner, Reference maps of human ES and iPS cell variation enable high-throughput characterization of pluripotent cell lines. *Cell* **144**, 439–452 (2011).
36. G. L. Boulting, E. Kiskinis, G. F. Croft, M. W. Amoroso, D. H. Oakley, B. J. Wainger, D. J. Williams, D. J. Kahler, M. Yamaki, L. Davidow, C. T. Rodolfa, J. T. Dimos, S. Mikkilineni, A. B. MacDermott, C. J. Woolf, C. E. Henderson, H. Wichterle, K. Eggan, A functionally characterized test set of human induced pluripotent stem cells. *Nat. Biotechnol.* **29**, 279–286 (2011).
37. E. Dick, S. Kalra, D. Anderson, V. George, M. Ritso, S. H. Laval, R. Barresi, A. Aartsma-Rus, H. Lochmuller, C. Denning, Exon skipping and gene transfer restore dystrophin expression in human induced pluripotent stem cells-cardiomyocytes harboring DMD mutations. *Stem Cells Dev.* **22**, 2714–2724 (2013).
38. J. G. Doench, E. Hartenian, D. B. Graham, Z. Tothova, M. Hegde, I. Smith, M. Sullender, B. L. Ebert, R. J. Xavier, D. E. Root, Rational design of highly active sgRNAs for CRISPR-Cas9-mediated gene inactivation. *Nat. Biotechnol.* **32**, 1262–1267 (2014).
39. E. M. McNally, J. R. Kaltman, D. W. Benson, C. E. Canter, L. H. Cripe, D. Duan, J. D. Finder, W. J. Groh, E. P. Hoffman, D. P. Judge, N. Kertesz, K. Kinnett, R. Kirsch, J. M. Metzger, G. D. Pearson, J. A. Rafael-Fortney, S. V. Raman, C. F. Spurney, S. L. Targum, K. R. Wagner, L. W. Markham; Working Group of the National Heart, Lung, and Blood Institute; Parent Project Muscular Dystrophy, Contemporary cardiac issues in Duchenne muscular dystrophy. Working group of the national heart, lung, and blood institute in collaboration with parent project muscular dystrophy. *Circulation* **131**, 1590–1598 (2015).
40. F. Kamdar, S. Das, W. Gong, A. Klaassen Kamdar, T. A. Meyers, P. Shah, J. M. Ervasti, D. Townsend, T. J. Kamp, J. C. Wu, M. G. Garry, J. Zhang, D. J. Garry, Stem cell-derived cardiomyocytes and beta-adrenergic receptor blockade in Duchenne muscular dystrophy cardiomyopathy. *J. Am. Coll. Cardiol.* **75**, 1159–1174 (2020).
41. A. Atmanli, D. Hu, F. E. Deiman, A. M. van de Vrugt, F. Cherbonneau, L. D. Black III, I. J. Domian, Multiplex live single-cell transcriptional analysis demarcates cellular functional heterogeneity. *eLife* **8**, e49599 (2019).
42. O. Chirikian, W. R. Goodyer, E. Dzilic, V. Serpooshan, J. W. Buikema, W. McKeithan, H. Wu, G. Li, S. Lee, M. Merk, F. Galdos, A. Beck, A. J. S. Ribeiro, S. Paige, M. Mercola, J. C. Wu, B. L. Pruitt, S. M. Wu, CRISPR/Cas9-based targeting of fluorescent reporters to human iPSCs to isolate atrial and ventricular-specific cardiomyocytes. *Sci. Rep.* **11**, 3026 (2021).
43. L. Han, Y. Li, J. Tchao, A. D. Kaplan, B. Lin, Y. Li, J. Mich-Basso, A. Lis, N. Hassan, B. London, G. C. L. Bett, K. Tobita, R. L. Rasmusson, L. Yang, Study familial hypertrophic cardiomyopathy using patient-specific induced pluripotent stem cells. *Cardiovasc. Res.* **104**, 258–269 (2014).
44. Y. Kuroda, S. Yuasa, Y. Watanabe, S. Ito, T. Egashira, T. Seki, T. Hattori, S. Ohno, M. Kodaira, T. Suzuki, H. Hashimoto, S. Okata, A. Tanaka, Y. Aizawa, M. Murata, T. Aiba, N. Makita, T. Furukawa, W. Shimizu, I. Kodama, S. Ogawa, N. Kokubun, H. Horigome, M. Horie, K. Kamiya, K. Fukuda, Flecainide ameliorates arrhythmogenicity through NCX flux in Andersen-Tawil syndrome-iPS cell-derived cardiomyocytes. *Biochem. Biophys. Rep.* **9**, 245–256 (2017).
45. C. Long, L. Amoasii, A. A. Mireault, J. R. McAnally, H. Li, E. Sanchez-Ortiz, S. Bhattacharyya, J. M. Shelton, R. Bassel-Duby, E. N. Olson, Postnatal genome editing partially restores dystrophin expression in a mouse model of muscular dystrophy. *Science* **351**, 400–403 (2016).
46. C. E. Nelson, C. H. Hakim, D. G. Ousterout, P. I. Thakore, E. A. Moreb, R. M. Castellanos Rivera, S. Madhavan, X. Pan, F. A. Ran, W. X. Yan, A. Asokan, F. Zhang,

D. Duan, C. A. Gersbach, In vivo genome editing improves muscle function in a mouse model of Duchenne muscular dystrophy. *Science* **351**, 403–407 (2016).
47. N. E. Bengtsson, J. K. Hall, G. L. Odom, M. P. Phelps, C. R. Andrus, R. D. Hawkins, S. D. Hauschka, J. R. Chamberlain, J. S. Chamberlain, Muscle-specific CRISPR/Cas9 dystrophin gene editing ameliorates pathophysiology in a mouse model for Duchenne muscular dystrophy. *Nat. Commun.* **8**, 14454 (2017).
48. H. Nishimasu, X. Shi, S. Ishiguro, L. Gao, S. Hirano, S. Okazaki, T. Noda, O. O. Abudayyeh, J. S. Gootenberg, H. Mori, S. Oura, B. Holmes, M. Tanaka, M. Seki, H. Hirano, H. Aburatani, R. Ishitani, M. Ikawa, N. Yachie, F. Zhang, O. Nureki, Engineered CRISPR-Cas9 nuclease with expanded targeting space. *Science* **361**, 1259–1262 (2018).
49. P. Tornabene, I. Trapani, R. Minopoli, M. Centrulo, M. Lupo, S. de Simone, P. Tiberi, F. Dell'Aquila, E. Marrocco, C. Iodice, A. Iuliano, C. Gesualdo, S. Rossi, L. Giaquinto, S. Albert, C. B. Hoyng, E. Polishchuk, F. P. M. Cremers, E. M. Surace, F. Simonelli, M. A. De Matteis, R. Polishchuk, A. Auricchio, Intein-mediated protein trans-splicing expands adeno-associated virus transfer capacity in the retina. *Sci. Transl. Med.* **11**, eaav4523 (2019).
50. D. Duan, Y. Yue, J. F. Engelhardt, Expanding AAV packaging capacity with trans-splicing or overlapping vectors: A quantitative comparison. *Mol. Ther.* **4**, 383–391 (2001).
51. C. L. Bladen, D. Salgado, S. Monges, M. E. Foncuberta, K. Kekou, K. Kosma, H. Dawkins, L. Lamont, A. J. Roy, T. Chamova, V. Guergueltcheva, S. Chan, L. Korngut, C. Campbell, Y. Dai, J. Wang, N. Barišić, P. Brabec, J. Lahdetie, M. C. Walter, O. Schreiber-Katz, V. Karcagi, M. Garami, V. Viswanathan, F. Bayat, F. Buccella, E. Kimura, Z. Koeks, J. C. van den Bergen, M. Rodrigues, R. Roxburgh, A. Lusakowska, A. Kostera-Pruszczyk, J. Zimowski, R. Santos, E. Neagu, S. Artemieva, V. M. Rasic, D. Vojinovic, M. Posada, C. Bloetzer, P.-Y. Jeannet, F. Joncourt, J. Díaz-Manera, E. Gallardo, A. A. Karaduman, H. Topaloğlu, R. E. Sherif, A. Stringer, A. V. Shatillo, A. S. Martin, H. L. Peay, M. I. Bellgard, J. Kirschner, K. M. Flanigan, V. Straub, K. Bushby, J. Verschuuren, A. Aartsma-Rus, C. Béroud, H. Lochmüller, The TREAT-NMD DMD Global Database: Analysis of more than 7,000 Duchenne muscular dystrophy mutations. *Hum. Mutat.* **36**, 395–402 (2015).
52. A. M. Chakrabarti, T. Henser-Brownhill, J. Monserrat, A. R. Poetsch, N. M. Luscombe, P. Scaffidi, Target-specific precision of CRISPR-mediated genome editing. *Mol. Cell* **73**, 699–713.e6 (2019).
53. T. Aida, J. J. Wilde, L. Yang, Y. Hou, M. Li, D. Xu, J. Lin, P. Qi, Z. Lu, G. Feng, Prime editing primarily induces undesired outcomes in mice. *bioRxiv* 2020.08.06.239723 (2020).
54. J. M. Goldstein, M. Tabebordbar, K. Zhu, L. D. Wang, K. A. Messemer, B. Peacker, S. Ashrafi Kakhki, M. Gonzalez-Celeiro, Y. Shwartz, J. K. W. Cheng, R. Xiao, T. Barungi, C. Albright, Y.-C. Hsu, L. H. Vandenberghe, A. J. Wagers, In situ modification of tissue stem and progenitor cell genomes. *Cell Rep.* **27**, 1254–1264.e7 (2019).
55. J. B. Kwon, A. R. Ettyreddy, A. Vankara, J. D. Bohning, G. Devlin, S. D. Hauschka, A. Asokan, C. A. Gersbach, In vivo gene editing of muscle stem cells with adeno-associated viral vectors in a mouse model of Duchenne muscular dystrophy. *Mol. Ther. Methods Clin. Dev.* **19**, 320–329 (2020).
56. F. A. Ran, P. D. Hsu, J. Wright, V. Agarwala, D. A. Scott, F. Zhang, Genome engineering using the CRISPR-Cas9 system. *Nat. Protoc.* **8**, 2281–2308 (2013).
57. M. G. Kluesner, D. A. Nedveck, W. S. Lahr, J. R. Garbe, J. E. Abrahante, B. R. Webber, B. S. Moriarity, EditR: A method to quantify base editing from sanger sequencing. *CRISPR J.* **1**, 239–250 (2018).
58. E. K. Brinkman, T. Chen, M. Amendola, B. van Steensel, Easy quantitative assessment of genome editing by sequence trace decomposition. *Nucleic Acids Res.* **42**, e168 (2014).
59. C. A. Schneider, W. S. Rasband, K. W. Eliceiri, NIH Image to ImageJ: 25 years of image analysis. *Nat. Methods* **9**, 671–675 (2012).
60. A. Briguet, I. Courdier-Fruh, M. Foster, T. Meier, J. P. Magyar, Histological parameters for the quantitative assessment of muscular dystrophy in the mdx-mouse. *Neuromuscul. Disord.* **14**, 675–682 (2004).
61. P. W. Burridge, E. Matsa, P. Shukla, Z. C. Lin, J. M. Churko, A. D. Ebert, F. Lan, S. Diecke, B. Huber, N. M. Mordwinkin, J. R. Plews, O. J. Abilez, B. Cui, J. D. Gold, J. C. Wu, Chemically defined generation of human cardiomyocytes. *Nat. Methods* **11**, 855–860 (2014).

Acknowledgments: We thank J. Cabrera for graphics, J. M. Shelton for performing immunohistochemistry and H&E staining, Y. Zang and the Boston Children's Hospital Viral Core for AAV production, the Sanger Sequencing Core at McDermott Center at the University of Texas Southwestern Medical Center for sequencing services, and Y.-L. Min and Y. Zhang for constructive advice. We are grateful to S. Hauschka (University of Washington) for providing the muscle-specific CK8e promoter. **Funding:** This work was supported by funds from NIH (HL-130253, AR-071980, and AR-067294), the Senator Paul D. Wellstone Muscular Dystrophy Specialized Research Center (HD-087351), Cancer Prevention and Research Institute of Texas (RP200103), and the Robert A. Welch Foundation (grant 1-0025 to E.N.O.). **Author contributions:** F.C., A.C.C., and H.L. designed the experiments and the genome editing strategies, cloned sgRNAs, and performed sgRNA screening and data analysis; F.C. and A.C.C. performed AAV injections and animal studies; F.C., A.C.C., and C.R.-C. generated ΔEx51 iPSCs and performed iPSC culture and nucleofection experiments; E.S.-O. performed Western blots, immunohistochemistry, and imaging; A.A. performed iPSC culture, calcium-cycling experiments on cardiomyocytes, and data analysis; A.A.M. performed tissue processing; H.L. and A.A.M. performed DNA and RNA extraction, PCR, and off-target analysis experiments; and F.C., A.C.C., H.L., N.L., R.B.-D., and E.N.O. wrote and edited the manuscript. **Competing interests:** R.B.-D. and E.N.O. are consultants for Exonics Therapeutics/Vertex Genetic Therapies. The other authors declare that they have no competing interests. **Data and materials availability:** All data needed to evaluate the conclusions in the paper are present in the paper and/or the Supplementary Materials. Additional data related to this paper may be requested from the authors.

Submitted 8 January 2021
Accepted 15 March 2021
Published 30 April 2021
10.1126/sciadv.abg4910

Citation: F. Chemello, A. C. Chai, H. Li, C. Rodriguez-Caycedo, E. Sanchez-Ortiz, A. Atmanli, A. A. Mireault, N. Liu, R. Bassel-Duby, E. N. Olson, Precise correction of Duchenne muscular dystrophy exon deletion mutations by base and prime editing. *Sci. Adv.* **7**, eabg4910 (2021).